Preprints of the 21st IFAC World Congress (Virtual)
Berlin, Germany, July 12-17, 2020

Extended Kalman Filter based Estimation of the State of Charge of Lithium-Ion cells using a Switched Model ⋆

Bikky Routh * **Desham Mitra** * **Amit Patra** *
Siddhartha Mukhopadhyay *

* *Department of Electrical Engineering , Indian Institute of Technology Kharagpur, West Bengal, India, 721302*
(e-mail: bikkyrouthee@iitkgp.ac.in, ddesham@iitkgp.ac.in, amit@ee.iitkgp.ac.in, smukh@ee.iitkgp.ac.in)

Abstract: The State of Charge (SoC) is one of the important quantities estimated by the Battery Management System (BMS) of Lithium-ion cells. However, the hysteresis effect and flat SoC-OCV nature of Lithium Iron Phosphate (LFP) battery complicate the SoC estimation. This paper proposes a novel switched model to successfully capture the hysteresis phenomena and enhance the accuracy of SoC estimation of LFP cells. The model is switched between charge and discharge modes, where the current direction decides the mode. The model parameters are functions of SoC and the switched mode. The parameters are estimated from Pulse Charge Data (PCD) and Pulse Discharge Data (PDD) using a Successive Recursive Least Square (SRLS) technique. The SRLS algorithm ensures sufficiency of excitation by capturing only the transient response of each pulse. Using the proposed model, SoC estimation is carried out using the Extended Kalman Filter (EKF). The proposed approach is validated by a real drive cycle data which is widely used to test vehicle performance. The study has been carried out on $LiFePO_4$ pouch cell with a nominal capacity of 20Ah and a nominal voltage of 3.3V and experiments are performed using the Biologic (BCS-815) battery testing equipment.

Keywords: Battery model, Extended Kalman Filter (EKF), Hysteresis, LFP pouch cell, Successive Recursive Least Square (SRLS), State of Charge (SoC).

1. INTRODUCTION

1.1 Motivation

Lithium-ion batteries (LIBs) are used in grid applications, transportation, and data centers due to their advantages like high specific energy and power densities, long cycle life, and high charge efficiency. Commercially, LIBs are available in various cell chemistries like Lithium Nickel Cobalt Aluminium Oxide (NCA), Lithium Manganese Oxide (LMO), Lithium Iron Phosphate (LFP) etc, (Horiba (2014)). However, among all the chemistries, lithium iron phosphate $LiFePO_4$ or LFP has the best trade off among the cost, the power and energy densities, and safety (Tredeau and Salameh (2009)). Battery Management System (BMS) has also gained importance in order to ensure a long and safe battery life (Cheng et al. (2010)). Typically the open circuit voltage (OCV) of the battery is measured and its relationship with the SoC is utilized to estimate the latter.

1.2 Review of Modeling of LFP cell and SoC Estimation

Fundamentally, there are two kinds of cell models, namely, Physics-Based Model and Equivalent Circuit Model (ECM) (Barcellona and Piegari (2017)). The ECM is considered to be more appropriate model, as it has a lower modeling complexity compared to an electrochemical model and can replicate the behaviour of the battery reasonably well under the simplifying assumptions. LFP cell is being a prominent one among all other cell chemistries, however, has some limitations. For example, the operating voltage range of LFP cell is lower (2.6V - 3.65V), and it also exhibits an almost flat Open Circuit Voltage (OCV) from 20% and 80% SoC range. However, this makes it difficult to estimate the SoC, which is expressed as a function of the OCV. Apart from the above, the LFP cell exhibits higher hysteresis i.e, at the same SoC, the OCV differs considerably between charge and discharge cycle. The lowest hysteresis voltage was found in the LTO cell (16mV) while the maximum was observed in the LFP cell (38mV) (Barai et al. (2015)). Therefore, the flat OCV nature and the effect of hysteresis on $LiFePO_4$ cell necessitates further research in this area.

Dong et al. (2016) has proposed an online Invariant Imbedding Method (IIM) to estimate the SoC and the parameters encapsulating the effect of the hysteresis of the LFP cell. Marongiu et al. (2016) has investigated

⋆ It is gratefully acknowledged that this research is partially supported by the project HEV of SRIC IIT Kharagpur which is jointly funded by TATA Motors and Govt. of India under UAY scheme.

in detail the hysteresis factor of the LFP cell, where the dependency of OCV (minor and major loop) on C-Rate, temperature, aging and short term memory has been studied and it is found that the C-Rate and temperature do not influence the hysteresis behaviour of the LFP cell. Zhao and de Callafon (2016) has modelled the non-linear power delivery dynamics and also the minor hysteresis loops using the Takacs hysteresis model for LFP battery. The hysteresis effect on LFP battery is well formulated by Adaptive Discrete Preisach Model (ASPM) (Zhu et al. (2015)). Baronti et al. (2014) has used two different techniques to model the hysteresis of LFP, one being the One State Hysteresis (OSH) technique, where the relation between SoC and OCV is represented by a first order relaxation equation and the other uses the conventional Preisach Model based on Everett Function. However, in both the techniques a heuristic method is used to obtain the parameters of relaxation equation.

Coulomb Counting (CC) (Pang et al. (2001)) is the conventional method of SoC estimation based on current integration. However, direct integration of current without any provision for minimizing the error in the estimation often leads to large error in SoC. Hence, a closed loop method is used to estimate the SoC, using Kalman filter (KF) technique (Piller et al. (2001)) . Plett (2004) has given a benchmark solution for estimating SoC using an Extended Kalman Filter (EKF). The comparative study of SoC estimation using EKF, Unscented Kalman Filter (UKF) and Particle Filter is given in Mitra and Mukhopadhyay (2018). (Kim (2006);Malkhandi (2006)) has estimated SoC based on Sliding Mode Observer (SMO) and fuzzy logic respectively, however in these methods, cell modeling needs to be more perfect and SMO based SoC estimation is affected by the chattering phenomenon.

1.3 Key Contributions

Although considerable work has been carried out in this field, there are several limitations in the existing approaches. Hysteresis is one of the prime factors which influences the LFP cell model. The existing methods have addressed the issue of hysteresis at the cost of very complex, sensitive experiments. Also, the modeling of hysteresis has added an extra hysteresis state on the battery model, which has led to the modeling complexity and also increase in the computational time. In this paper, the hysteresis effect of the LFP battery is captured by proposing a switched model, which is explained in subsection 4.2. The proposed switched model has two operating modes, namely, Charge Mode (CM) and Discharge Mode (DM). The parameters under Charge Mode are estimated from Pulse Charge Data (PCD) and those of the Discharge Mode from Pulse Discharge Data (PDD). An Extended Kalman Filter (EKF) is used to estimated the SoC. The EKF algorithm switches accordingly to CM or DM based on the current direction.

A Successive Recursive Least Square (SRLS) based parameter identification method is formulated and implemented at different SoC values, so as to ensure the sufficiency of excitation and this is realized by selectively extracting the portion of the data that contains significant transient parts. Moreover, a look-up table based mapping between the estimated parameters and its corresponding SoC has been developed.

2. BATTERY MODELING AND PARAMETER ESTIMATION

2.1 Battery Model

The cell model is represented by a one time constant equivalent circuit model which is shown in Fig. 1. V_{oc} represents

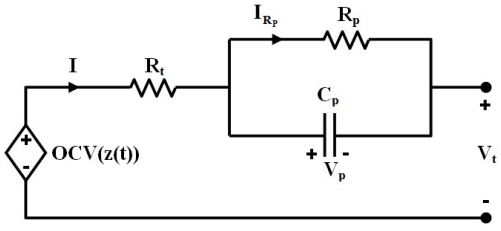

Fig. 1. An equivalent circuit model

the Open Circuit Voltage (OCV) which is a function of State of Charge (z(t)), as the voltage of a cell depends upon the charge condition. R_t represents the equivalent series resistance of the cell. The diffusion voltage in a cell is replicated by the combination of resistor-capacitor (R_p, C_p) in a model where as, V_t represents the terminal voltage of a cell. From the equivalent circuit diagram

$$\begin{aligned} V_t &= V_{oc} - I_{Rp}R_p - IR_t \\ V_d &= V_t - V_{oc} \\ V_d(s) &= -I(s)\left(R_t(s) + \frac{R_p}{1+sR_pC_p}\right) \end{aligned} \tag{1}$$

(1) is represented in the Laplace Transform domain, where I is the input current and V_d is the dynamic voltage. We transform it to the discrete domain by using the forward transformation method shown below (2)

$$s = \frac{1-z^{-1}}{Tz^{-1}} \tag{2}$$

where T is a the sampling time and z is the complex operator in the discrete domain. We thereby obtain the discrete transform function of the model as shown below.

$$G(z^{-1}) = \frac{R_t + \frac{TR_p}{R_pC_p+T} - \frac{R_tR_pC_p}{R_pC_p+T}z^{-1}}{1 - \frac{R_pC_p}{R_pC_p+T}z^{-1}}$$

$$G(z^{-1}) = \frac{b_0 + b_1z^{-1}}{1 + a_1z^{-1}} \tag{3}$$

where,

$$\begin{aligned} a_1 &= \frac{-R_pC_p}{R_pC_p+T} \\ b_0 &= R_t + \frac{TR_p}{T+R_pC_p} \\ b_1 &= \frac{R_tR_pC_p}{R_pC_p+T} \end{aligned}$$

Finally,

$$V_d(k) = -a_1V_d(k-1) + b_0I(k) + b_1I(k-1) \tag{4}$$

(4) represents the Autoregressive Moving Average (ARMA) model which is to be used for the parameter identification.

2.2 Parameter Estimation

A SRLS technique is framed for the parameter identification, where each current pulse is applied to the ARMA model in two steps. For PDD, first the rising edge then the falling edge of a pulse is applied as shown in Fig. 2. (a). In this case, parameter estimates of the rising edge are used as initial parameters value for the falling edge. The falling edge estimates are taken as final parameter estimates. The duration of the falling edge is taken to be 300 seconds before and 300 seconds after the edge. For the rising edge, it is 200 seconds before and 240 seconds after the edge. This same procedure is implemented for rest of the pulses in PDD. For PCD, first the falling edge then the rising edge is applied as shown in Fig. 2. (b). On the other hand, for PCD, the initial value of the rising edge is obtained from the estimates parameters of the falling edge. For PCD, the duration of the rising edge is taken 180 seconds before and 240 seconds after the edge and for falling edge its 300 seconds before and 240 seconds after the edge.

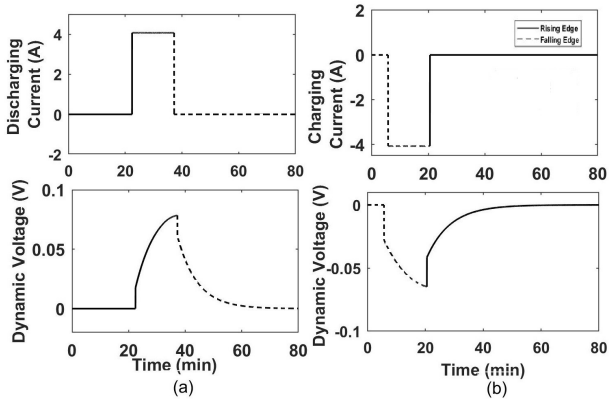

Fig. 2. Input and output pulse of PDD and PCD

The parameters (a_1, b_0, b_1) are estimated using SRLS technique. $\varphi(k) = [-V_d(k), I(k), I(k-1)]^T$ is the input vector with current $I(k)$ as input and dynamic voltage $V_d(k)$ as output.
$\hat{\theta}(k) = [a_1(k), b_0(k), b_1(k)]$ is the coefficient vector.
The error is expressed as,

$$e(k+1) = V_d(k+1) - \varphi^T(k+1)\hat{\theta}(k) \tag{5}$$

The update gain $L(k)$ is given by :

$$L(k) = \frac{P(k)\varphi(k+1)}{I + \varphi^T(k+1)P(k)\varphi(k+1)} \tag{6}$$

The coefficient vector $\hat{\theta}(k)$ is calculated by

$$\hat{\theta}(k+1) = \hat{\theta}(k) + L(k)e(k+1) \tag{7}$$

The covariance matrix $P(k)$ is the estimated coefficient vector $\hat{\theta}(k)$ which is given below.

$$P(k+1) = P(k)[I - L(k)\varphi^T(k+1)] \tag{8}$$

P is 3×3 diagonal matrix and I is 3×3 Identity matrix

3. EXPERIMENTAL SET-UP AND DATA COLLECTION

Experiments have been carried out on Lithium Iron Phosphate (LFP) rechargeable pouch cell of nominal capacity

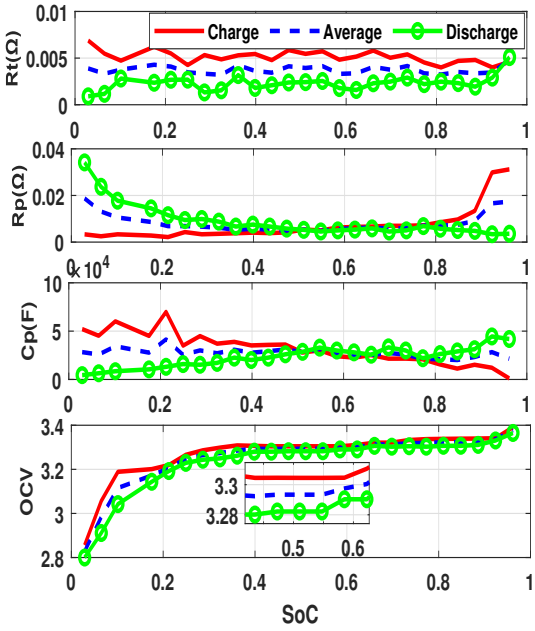

Fig. 3. Parameter variation w.r.t. SoC for Charge-Discharge

20Ah and nominal voltage of 3.3 V to validate the above approach. The experiments was conducted in Biologic (BCS-815) battery testing equipment shown in Fig. 4, having the current range of ±15A, voltage range from 0 to 9V and measurement resolution of 40µV. All the experiments were carried out at room temperature of 25°C to minimize the temperature effect.

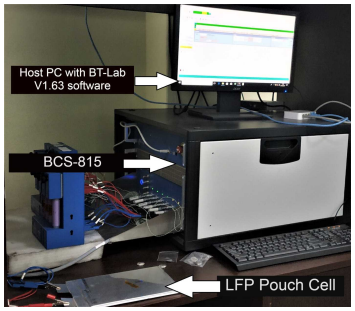

Fig. 4. The Experimental set-up

Initially, the cell was fully discharged with a Constant Current profile till the voltage reached its minimum prescribed limit of 2.6V (0% SoC). After that, a Pulse Charge Test (PCT) was conducted to obtained PCD, were the cell was charged with a current pulse of 4A for 15 min, so that 5% of SoC is reached and the cell was given rest for 75 min, to retain its thermal equilibrium. This process continued until the SoC of the cell reached its maximum voltage of 3.6V (100% SoC). Similarly, Pulse Discharge Test (PDT) was conducted to obtained PDD. The cell was discharged with 4A current for 15 min, so that 5% charge is decreased, after that, rest for 75 min was given. This test continued till the voltage of the cell reached 2.6V (0% SoC). The relaxation time of 75 min is to ensure that the cell voltage reaches its OCV.

In order to experimentally validate the proposed model, a test for the CYC_ARB02 drive cycle [1] was conducted, which is widely used to test vehicle performance. At first the cell was fully charged till maximum voltage of 3.6V (100% SoC) and then it was discharged till 68% SoC by constant current of 3A. When the SoC of the cell reached 68%, the CYC_ARB02 drive cycle current profile was applied to the cell, till the SoC reached 60%.

4. MODEL VALIDATION

4.1 Average Model

In order to study the hysteresis dynamics, the battery is first modelled as an average model. The Average model signifies that the average of parameters (Par_{avg}) estimated from PCD and PDD data are used for modeling. The average parameters Par_{avg} are calculated using (9), where Par_{avg} implies ($R_{t_{avg}}, R_{p_{avg}}, C_{p_{avg}}, OCV_{avg}$), Par_{chg} infer charging parameters ($R_{t_{chg}}, R_{p_{chg}}, C_{p_{chg}}, OCV_{chg}$) which is a function of SoC while charging (SoC_{chg}) and the discharging parameters ($R_{t_{dchg}}, R_{p_{dchg}}, C_{p_{dchg}}, OCV_{dchg}$) are functions of SoC while discharging (SoC_{dchg}).

$$Par_{avg} = \frac{Par_{chg}(SoC_{chg}) + Par_{dchg}(SoC_{dchg})}{2} \quad (9)$$

$$V_t(k) = V_{oc}(z(k)) - I_{Rp}(k)R_p) - I(k)R_t \quad (10)$$

The plot of the parameter variation w.r.t. SoC during

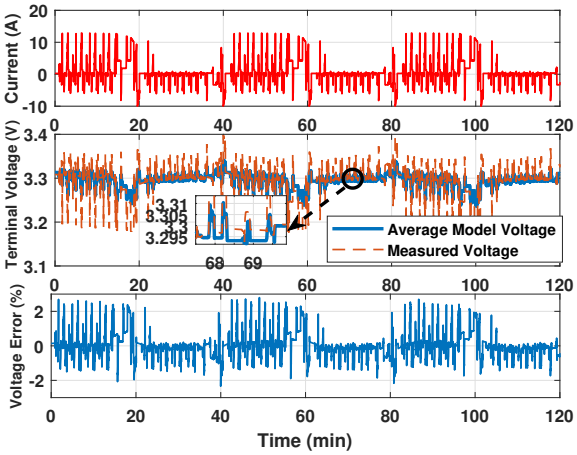

Fig. 5. Comparison between measured and average model voltage

charging, discharging and their average is shown in Fig. 3, where the hysteresis nature of LFP cell in SoC-OCV curve is shown. The equation which governs the model output voltage is given in (10). The cell model is validated by CYC_ARB02 drive cycle. The CYC_ARB02 drive cycle current signal, comparison of measured and average model output voltage and, error in the average model are shown in Fig. 5.

[1] http://read.pudn.com/downloads334/sourcecode/math/1466859/ADVISOR2002/data/drive_cycle/CYC_ARB02.m__.htm

4.2 Proposed Model: Switched Model

The proposed model is termed as the switched model. As the name depicts switch, it means switching between the Charge and the Discharge Mode and the switching is governed by the input current. The Stateflow diagram is shown in Fig. 6 for the charge and discharge modes, where I and k are the input current and time instant respectively. When current $I(k)$ is positive, then the state i.e, SoC will be on discharge mode. There are two conditions when the state will be in the discharge mode, namely
(i) When $I(k)$ is 0 and $I(k-1)$ is 0
(ii) When $I(k)$ is 0 and $I(k-1)$ is positive.
In the Discharge Mode, the estimated parameters for discharge mode $P_{dchg}(SoC_{dchg})$ works, which will in turn approximates the hysteresis effect. As soon as I is negative, the state will switch into the Charge Mode, where the estimated charge parameters $P_{chg}(SoC_{chg})$ works for SoC estimation.
When the state is in charge mode it will stay in the charge mode under the conditions
(i) When $I(k)$ is 0 and $I(k-1)$ is 0.
(ii) When $I(k)$ is 0 and $I(k-1)$ is negative.

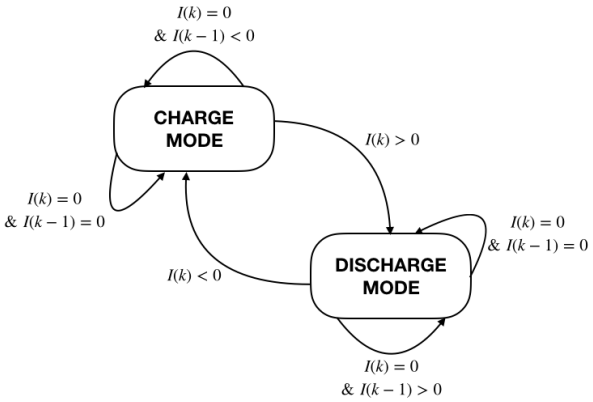

Fig. 6. Stateflow diagram of the proposed switched model

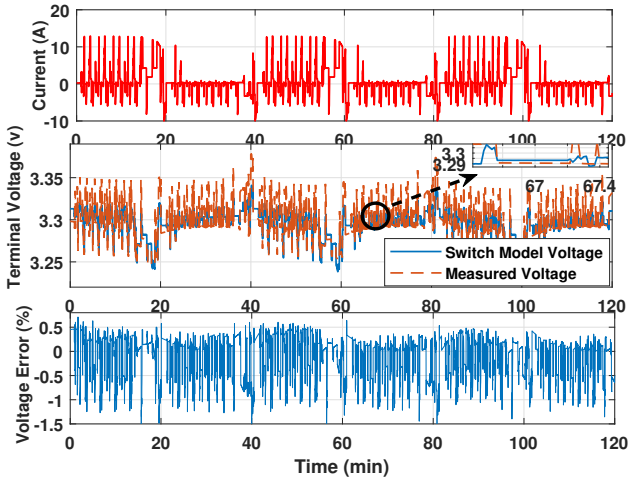

Fig. 7. Comparison between measured and switched model voltage

In Fig. 7, the percentage voltage error lies within -1% to 0.5%. Therefore, it signifies that the switched model has

captured the hysteresis phenomena quite well which leads to improvement of the cell model. The model developed is used in the SoC estimation of a cell using EKF framework which is explained in the subsequent section.

5. STATE OF CHARGE ESTIMATION USING AVERAGE AND SWITCHED MODELS

The EKF framework is used to estimated the SoC using both the models. The EKF technique improves the accuracy of estimation by incorporating the measurement and process noise in estimation. Also, the reliance on the initial SoC is lightened using EKF. The states of the cell are State of Charge ($z(t)$) and the current (I_{R_p}) through the resistor (R_p) which is shown in (11) and (12). The equation governing the output (V_t) is given by (13).

$$z(k+1) = z(k) - \frac{\eta \Delta t}{Q} I(k) + w_1(k) \tag{11}$$

$$I_{Rp}(k+1) = I_{Rp}(k) e^{-\frac{\Delta t}{R_p C_p}} + I(k)(1 - e^{-\frac{\Delta t}{R_p C_p}}) + w_2(k). \tag{12}$$

$$V_t(k) = V_{oc}(z(k)) - I_{Rp}(k) R_p - I(k) R_t + v(k) \tag{13}$$

where, Q is the nominal capacity, $I(k)$ is the true cell current and $w_1(k)$ and $w_2(k)$ are process noise of $z(t)$ and I_{R_p} respectively. Where, $V_t(k)$ and $v(k)$ are the terminal voltage and the voltage-sensor measurement noise respectively. η is coulombic efficiency which is taken 1 for both charge and discharge modes. As EKF works for mild nonlinearities. Therefore, the above equations are transformed into Jacobian Matrices by Jacobian linearisation method which is shown below.

$$\hat{A} = \begin{pmatrix} \frac{\partial z(k+1)}{\partial z(k)} & \frac{\partial z(k+1)}{\partial I_{Rp}(k)} \\ \frac{\partial I_{Rp}(k+1)}{\partial z(k)} & \frac{\partial I_{Rp}(k+1)}{\partial I_{Rp}(k)} \end{pmatrix}, \hat{B} = \begin{pmatrix} \frac{\partial z(k+1)}{\partial w_1(k)} \\ \frac{\partial I_{Rp}(k+1)}{\partial w_2(k)} \end{pmatrix}$$

$$\hat{C} = \begin{pmatrix} \frac{\partial V_t(k)}{\partial z(k)} & \frac{\partial V_t(k)}{\partial I_{Rp}(k)} \end{pmatrix}, \hat{D} = \frac{\partial V_t(k)}{\partial v(k)}$$

Finally,

$$\hat{A} = \begin{pmatrix} 1 & 0 \\ 0 & e^{-\frac{\Delta t}{R_p C_p}} \end{pmatrix}, \hat{B} = \begin{pmatrix} 1 \\ 1 \end{pmatrix} \tag{14}$$

$$\hat{C} = \begin{pmatrix} \frac{\partial V_{oc}(z(k))}{\partial z(k)} & -R_p \end{pmatrix}, \hat{D} = 1 \tag{15}$$

where, $\hat{A}$ is 2×2 system matrix , $\hat{B}$ is 2×1 input matrix, $\hat{C}$ is 1×2 output matrix and $\hat{D}$ is 1×1 feed-forward matrix. An average model is modelled based on the average of parameters (Par_{avg}) estimated using SRLS technique from PCD and PDD data. The estimated average parameter is calculated based on (9). An EKF algorithm is applied to the model and SoC is estimated.
The switched model consists of a charge mode and a discharge mode. Therefore, for a SoC estimation, either of the one, CM or DM will work at a time. A lookup table model for CM and DM is developed separately based on their respective mode parameters. The novelty of the model is that, the EKF algorithm framed for a SoC estimation switches to either of the mode (CM or DM) based on the current direction. If the current is positive, the EKF algorithm estimate the SoC for discharge mode and for negative current it will switch back to charge mode and estimates SoC. In this way, the hysteresis phenomena of LFP cell is captured by the proposed switched model, which further improves the SoC estimation. The complete EKF algorithm is explained in (Plett (2004)).

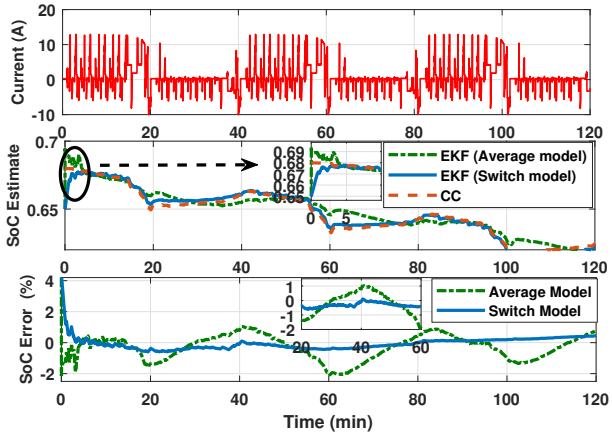

Fig. 8. SoC estimation using EKF for switched and average model with their error plots

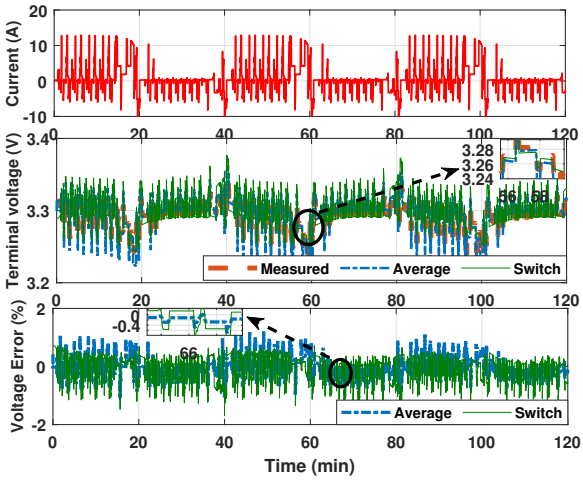

Fig. 9. Comparison of estimated terminal voltage using EKF for switched model and average model with their error plots

6. SIMULATION RESULTS AND DISCUSSIONS

The validation of the average and switched model is done by CYC_ARB02 drive cycle profile, which incorporates the current variations ranging from ± 10A. Fig 5 and 7 show current profile of CYC_ARB02 drive cycle, average and switched model voltage in comparison with true voltage and their error band respectively. Figure 5 shows the percentage modeling error of average model lies in a band of ±2%. In the switched model, the voltage error is much lower, i.e, in the band of ±0.5%, shown in Fig. 7. Here, the error percentage is defined as follows.

$$Error(\%) = \frac{Measured - Estimated}{Measured} \times 100 \tag{16}$$

The initial true SoC is known to be 68% from the data. To verify the convergence of EKF, the initial SoC is chosen as 63% for both the models. The value of initial states covariance (P), process noise covariance (Q) and the sensors noise covariance (R) were deliberately chosen by tuning to assure the best convergence of the EKF algorithm in both the models. The value of P, Q, and R were chosen as $P_0 = \begin{pmatrix} 0.11 & 0 \\ 0 & 0.11 \end{pmatrix}$, $Q = \begin{pmatrix} 10^{-10} & 0 \\ 0 & 10^{-10} \end{pmatrix}$ and $R = 2$ for switched model. Whereas, for average model the values were chosen as $P_0 = \begin{pmatrix} 0.11 & 0 \\ 0 & 0.11 \end{pmatrix}$, $Q = \begin{pmatrix} 10^{-8} & 0 \\ 0 & 10^{-8} \end{pmatrix}$ and $R = 2.5$. The simulation results are shown in Fig. 8 and 9. Figure 8 illustrates that the error in the beginning is due to the initial state error, after that the SoC convergence to its real value within 5 minutes in both the models. In the switched model, the SoC error is in the band of less then $\pm 0.5\%$, Whereas for the average model the error is in the band of $\pm 2\%$. Figure 9 shows the measured, switched and average model voltage and their respective voltage errors using EKF. The voltage errors for switched model lies between $\pm 0.5\%$. However, in the average model the error lies in the band of $\pm 1\%$. The error is calculated based on (16) in all the cases. The test results shows that the proposed model is able to approximates the hysteresis effect of LFP cell, leading to reduced modeling error and higher SoC accuracy.

7. CONCLUSION

In this paper, a new modeling approach of LFP cells is presented, which is termed as a Switched Model, to incorporate the effects of hysteresis and enhance the SoC accuracy. The SRLS algorithm is proposed for parameter identification. The SRLS ensures sufficiency of excitation and the whole transient response of each pulse is captured. The model was validated by a real CYC_ARB02 drive cycle. The results show that the switched model significantly decrease the errors ($<1\%$) between the switched model voltage and true voltage acquired from the experiment. The EKF framework is applied to estimate the cell SoC with the proposed model. The SoC error is in a band of $\pm 0.5\%$, which indicates considerable potential of the switched model.
The model accuracy can be further improved by incorporating the influence of temperature variation. Also, this work can be further extended to design an online bootstrap estimator, where the parameters for charge-discharge mode will be estimated online. The updated parameters would be used for SoC estimation in its respective mode based on current direction logic.

ACKNOWLEDGEMENTS

The authors would like to acknowledge Prof. S. B. Majumder of the Materials Science Center, IIT Kharagpur for providing the facility to carry out experimental work and giving many useful suggestions.

REFERENCES

Barai, A., Widanage, W.D., Marco, J., McGordon, A., and Jennings, P. (2015). A study of the open circuit voltage characterization technique and hysteresis assessment of lithium-ion cells. *Journal of Power Sources*, 295, 99–107.

Barcellona, S. and Piegari, L. (2017). Lithium ion battery models and parameter identification techniques. *Energies*, 10(12), 2007.

Baronti, F., Femia, N., Saletti, R., and Zamboni, W. (2014). Comparing open-circuit voltage hysteresis models for lithium-iron-phosphate batteries. In *IECON 2014-40th Annual Conference of the IEEE Industrial Electronics Society*, 5635–5640. IEEE.

Cheng, K.W.E., Divakar, B., Wu, H., Ding, K., and Ho, H.F. (2010). Battery-management system (BMS) and SOC development for electrical vehicles. *IEEE transactions on vehicular technology*, 60(1), 76–88.

Dong, G., Wei, J., Zhang, C., and Chen, Z. (2016). Online state of charge estimation and open circuit voltage hysteresis modeling of LiFePO4 battery using invariant imbedding method. *Applied Energy*, 162, 163–171.

Horiba, T. (2014). Lithium-ion battery systems. *Proceedings of the IEEE*, 102(6), 939–950.

Kim, I.S. (2006). The novel state of charge estimation method for lithium battery using sliding mode observer. *Journal of Power Sources*, 163(1), 584–590.

Malkhandi, S. (2006). Fuzzy logic-based learning system and estimation of state-of-charge of lead-acid battery. *Engineering Applications of Artificial Intelligence*, 19(5), 479–485.

Marongiu, A., Nußbaum, F.G.W., Waag, W., Garmendia, M., and Sauer, D.U. (2016). Comprehensive study of the influence of aging on the hysteresis behavior of a lithium iron phosphate cathode-based lithium ion battery–An experimental investigation of the hysteresis. *Applied energy*, 171, 629–645.

Mitra, D. and Mukhopadhyay, S. (2018). UKF Based Estimation of SOC and Core Temperature of a Lithium Ion Cell Using an Electrical Cell Model. In *2018 15th IEEE India Council International Conference (INDICON)*, 1–6.

Pang, S., Farrell, J., Du, J., and Barth, M. (2001). Battery state-of-charge estimation. In *Proceedings of the 2001 American control conference.(Cat. No. 01CH37148)*, volume 2, 1644–1649. IEEE.

Piller, S., Perrin, M., and Jossen, A. (2001). Methods for state-of-charge determination and their applications. *Journal of power sources*, 96(1), 113–120.

Plett, G.L. (2004). Extended Kalman filtering for battery management systems of LiPB-based HEV battery packs: Part 3. State and parameter estimation. *Journal of Power sources*, 134(2), 277–292.

Tredeau, F.P. and Salameh, Z.M. (2009). Evaluation of lithium iron phosphate batteries for electric vehicles application. In *2009 IEEE Vehicle Power and Propulsion Conference*, 1266–1270. IEEE.

Zhao, X. and de Callafon, R.A. (2016). Modeling of battery dynamics and hysteresis for power delivery prediction and SOC estimation. *Applied energy*, 180, 823–833.

Zhu, L., Sun, Z., Dai, H., and Wei, X. (2015). A novel modeling methodology of open circuit voltage hysteresis for LiFePO4 batteries based on an adaptive discrete Preisach model. *Applied energy*, 155, 91–109.